Wang et al. Journal of Biological Engineering (2025) 19:7
https://doi.org/10.1186/s13036-024-00471-y

Journal of Biological Engineering

RESEARCH Open Access

BCL-2 overexpression exosomes promote the proliferation and migration of mesenchymal stem cells in hypoxic environment for skin injury in rats

Ying Wang[1], Guang Li[1], Guofeng Li[1], Yutao Pan[1] and Zhongmin Liu[1*]

Abstract

Objective The direction of this study was to detect and analyze the specific mechanism of anti-apoptosis in mesenchymal stem cells (MSCs) cells caused by high expression of BCL2.

Methods Bioinformatics was completed in Link omics. GO analysis and KEGG analysis were carried out, and the grope tool of Link omics database was used to evaluate PPI information and other core path analysis information. The cultured cells were divided into MSC + normoxic group (MSCs were cultured in conventional medium, including 10% depleted serum of fetal bovine exosomes, 37 °C, 5% CO_2 and 95% air) and Exo-BCL-2 + MSC + normoxic group (a certain concentration of purified BCL-2 exosomes was co-cultured with MSC in conventional medium, 37 °C, 5% CO_2 and 95% air), Exo-BCL-2 + MSC + hypoxia group (a certain concentration of purified BCL-2 exosomes and MSC were co-cultured in hypoxia medium at 37 °C, 80% CO_2 and 20% air), MSC + hypoxia group (MSCs were cultured in hypoxia medium with 10% depleted serum of fetal bovine exosomes, 37 °C, 80% CO_2 and 20% air), exo WT + MSC + normoxic group (co-cultured with MSC in conventional medium at 37 °C, 5% CO_2 and 95% air) and exoWT + MSC + hypoxic group (co-cultured with MSC in hypoxic medium at 37 °C, 80% CO_2 and 20%). Cell proliferation ability was monitored by cell proliferation test. Cell migration test was used to check the migration capacity of MSCs. The expressions of apoptosis-related proteins BCL-2, caspase3 and caspase9, Runx2, ALP and PPAR-γ were analyzed by western blot. Tissue damage was scored by H&E and Ma Song trichrome staining. Masson staining was used to evaluate the collagen volume fraction of the wound. The expressions of KRT14, α-SMA, CD31 and PCNA in rat trauma tissues were analyzed by immunofluorescence staining. The horizontal of apoptosis-related proteins in skin lesions was checked by Western blot. The horizontal of inflammatory factors TNF-α and IL-6 in traumatic tissue of rats were detected by ELISA.

Results From KEGG's results, we can see that BCL2-2 was closely related to base excision and repair, cell cycle, steroid biosynthesis and other pathways. When cultured for 48h and 72h, the proliferation ability and migration number of MSCs in MSC + hypoxia group were lower than MSC + normoxic group, but the expressions of caspase3 and caspase9 were higher. The proliferation ability and migration number of MSCs in Exo-BCL-2 + MSC + hypoxia group and MSC + hypoxia group were lower than those in Exo-BCL-2 + MSC + normoxic group and MSC + normoxic group, and the horizontal of caspase3 and caspase9 were lower. Exo-BCL-2 + MSC + normoxic group increased

*Correspondence:
Zhongmin Liu
zhongminliu@finmail.com
Full list of author information is available at the end of the article

the proliferation capacity and migration number of MSCs, but decreased the expression of caspase3 and caspase9. Compared with Exo-BCL-2 + MSC + normoxia and Exo-BCL-2 + MSC + normoxia, the proliferation ability and migration quantity of MSCs in exo WT + MSC + normoxia and exo WT + MSC + hypoxia groups were lower, and the horizontal of caspase3 and caspase9 proteins was higher.

Conclusion Bioinformatics analysis shows that BCL2-2 plays a worthwhile role in the process of cell apoptosis and proliferation. Exosomes with high expression of BCL-2 can encourage the proliferation of MSC in hypoxic environment. The wound treated with MSCs-BCL-2 promotes the compose of new blood vessels and granulation tissue in the wound, the redifferentiation of epithelial cells and the remodeling of collagen, which has a high therapeutic prospect for chronic wounds and skin regeneration.

Keywords BCL-2 overexpression, Exosomes, Mesenchymal stem cells, Hypoxia-induced apoptosis

Background

These Extracellular vesicles (ev) are mainly divided into three categories depending on the diameter of ev, including exosomes, microcapsules and apoptotic bodies [1, 2]. It is worth noting that exosomes are little lipid bilayer vesicles with a diameter of 30–150 nm, which are derived from some biological fluids [3]. These nanocapsules contain many cell-specific protein and lipids, which have become a new intercellular communication system on the inner chamber of donor cells and the outer or inner chamber of recipient cells [4]. Exosomes are major signal transport body on cells and can also be used as paracrine pathways of parent cells. More and more evidences show that exosomes discharge their active material for substance transport through specific binding with target cells, thus regulating biological behavior. In addition, signal transmission is carried out through signal molecules on the surface of exosomes, and exosomes immediately play the role target cells through receptor-mediated interaction [5]. According to the current research, exosomes not only have broad application prospects as biomarkers, but also show clinical potential in tissue regeneration, which deserves our attention and efforts as free cell therapy [6]. A large amount of evidence shows that exosomes from stem cells have the potential to treat tissue repair and regeneration, including accelerating skin wound healing [7, 8].

MSCs have shown great underlying for wound healing, and have become one of the most promising substitutes for tissue regeneration, immunomodulation and promoting repair because of their more definite pluripotent differentiation potential, proliferation and growth, paracrine action, immunomodulation characteristics and better safety [9]. MSCs have the advantages of abundant resources, less trauma, less adverse reactions, expansibility [10]. The potential risk of low overall survival of MSCs implanted cells limits the clinical application of MSCs. In addition, the potential mechanism of MSCs' function remains to be clarified. More and more studies show that the potential role of MSCs mainly depends on the mechanism mediated by paracrine. This outcome is thought to occur through the secretion of a large number of substances [11]. Most interestingly, from paracrine MSCs, namely MSCs exosomes (MSCs-exosomes), play an unparalleled function as a mediator in intercellular communication. In view of the increase of research on MSCs-exosomes, the research related to MSCs-exosomes is raising [12, 13]. Publications on the use of MSCs- exos have shown effective treatment for many illness models [14, 15]. Therefore, in view of the accessibility and potential utility of MSCs-Exos in wound healing applications, it has aroused great interest. Skin injuries are common after accidental injuries. Therefore, shortening the healing time after skin/soft tissue injury and inhibiting scar formation are urgent clinical needs. Although many treatment attempts have promoted wound healing, the best treatment strategy is still under development [16]. It has been reported that local injection of exosomes secreted by human stem cells can encourage the multiplication of skin cells, wound closure of diabetes or burn wounds, which indicates that exosomes-based treatment is a promising wound healing method. In this study, BCL-2 exosomes were extracted from rat serum, and the mechanism of MSCs-BCL-2 in treating skin injury model was evaluated.

Materials and methods

KEGG and GO analysis

The data used in the analysis of DEGs came from the GEO database of NCBI, numbered GSE3467. The original chip data (CEL file) was preprocessed by R/Bioconductor package affy, including background correction and standardization. The RMA method was used, and then the difference of gene horizontal was tested by R/Bioconductor package limma software. The threshold of differential expression was 0.05. Multi MiR package software was used to forecast the miRNA-target relationship pair, and the threshold value was set to 35, which was predicted by at least three algorithms [17]. R/bioconductor

package cluster Profiler was used as KEGG pathway and GO enrichment analysis software.

Collection of HucMSCs source conditioned medium and isolation of extracellular vesicles

HucMSC Ex cells are in the logarithmic growth phase and have good growth status (long spindle shaped, small in size, fast in growth, clustered growth, and no obvious heterochromatic particles in the cytoplasm). P3 generation hucMSCs were extensively expanded in vitro to 10 cm2 dishes, and the cells were maintained in a-MEM complete culture medium containing 10% fetal bovine serum and double antibodies. When the cell growth fusion degree reached 50%～70% (about 5×105 cells), the cells were washed three times with PBS and replaced with 8 mL of a-MEM complete culture medium containing 10% fetal bovine serum, which had removed serum exosomes (4C100000 g centrifuged for 16 h). The cells were further cultured for 48 h, and the cell culture supernatant was collected. The same batch of hucMSCs comes from the supernatant, labeled with the collected algebra, date, and the initials of the collection personnel. In the collection of supernatant, different sterile vessels were used according to the number of passaged cells, including 15 mL, 50 mL, 100 mL, and 500 mL. The collected culture supernatant was stored in a −80 ℃ ultra-low temperature freezer for future use. Specific detailed steps: ① Thaw the cell supernatant in a −80 ℃ freezer, then centrifuge at 300 g at 4 ℃ for 10 min to remove complete cell precipitates. ② Centrifuge at 4 ℃ 2000 g for 10 min to remove dead cell sediment Centrifuge at 10,000 g at 4 ℃ for 30 min to remove cell debris and organelle components Subsequently, the supernatant was transferred to a 100 kDa MWCO ultrafiltration centrifuge tube and centrifuged at 4 ℃ 2000g for 30 min for appropriate concentration Transfer the concentrated solution to a 40 mL volumetric centrifuge tube, centrifuge at 4 ℃100,000 g for 3 h, discard the supernatant, and resuspend the hucMSC Ex precipitate in PBS Repeat the previous centrifugation step, discard the supernatant, resuspend hucMSC Ex precipitate in an appropriate volume of PBS, and let it stand overnight at 4 ℃. The dissolved hucMSC Ex solution was filtered through a 0.22 μ m sterile filter for sterilization and divided into 1.5 mL sterile EP tubes Finally, store hucMSC Ex in an −80C ultra-low temperature freezer for future use. The molecular markers (CD63, CD81) were verified to be correct, and the size of the extracellular vesicles was 40–100 nm with a purity of 100%. This study characterizes exons through exon labeling, which involves extracting sample DNA, capturing and enriching exons, and sequencing the captured exon regions using high-throughput sequencing technology. After obtaining sequencing data, bioinformatics analysis is performed, including data quality control, mutation detection, and identification and characterization of exon markers.

The detection results of BCL-2 marker in Exosome are shown in Fig. 1(a)

The article supplemented the steps of nano tracking analysis of extracellular vesicle quantity and fluid dynamic size, as well as the size and distribution of extracellular vesicles. The results of extracellular vesicle particle size analysis are as follows, with an average particle size of 80.82nm and a concentration of 1.35E+10 particles/mL

The measured OD562 of extracellular vesicle proteins were applied to the above formula for calculation, and the extracted extracellular vesicle protein concentrations were as follows: the protein concentration with lysis buffer was 0.4834785 μ g/μ L, and the original protein concentration was 0.604348125 μ g/μ L).

The molecular markers (CD63, CD81) were verified to be correct, and the size of the extracellular vesicles was 40–100 nm with a purity of 100%

Cell grouping

The cultured cells were divided into MSC + normoxic group (MSCs were cultured in conventional medium, including 10% depleted serum of fetal bovine exosomes, 37°C, 5% CO_2 and 95% air) and Exo-BCL-2 + MSC + normoxic group (a certain concentration of purified BCL-2 exosomes was co-cultured with MSC in conventional medium, 37 °C, 5% CO_2 and 95% air), Exo-BCL-2 + MSC + hypoxia group (a certain concentration of purified BCL-2 exosomes and MSC were co-cultured in hypoxia medium at 37°C, 80% CO_2 and 20% air), MSC + hypoxia group (MSCs were cultured in hypoxia medium with 10% depleted serum of fetal bovine exosomes, 37 °C, 80% CO_2 and 20% air), exo WT + MSC + normoxic group (co-cultured with MSC in conventional medium at 37°C, 5% CO_2 and 95% air) and exoWT + MSC + hypoxic group (co-cultured with MSC in hypoxic medium at 37°C, 80% CO_2 and 20%). Note: The hypoxic environment for the hypoxic group was set to 38 °C, 80% CO_2, and a 20% O_2 cell culture incubator.

Cell proliferation test

MSCs were inoculated at the ratio of 2×10^3 cells/well, and then co-cultured with a certain purified concentration of BCL-2 exosomes (whether added or not depended on the experimental grouping) for 48 h under

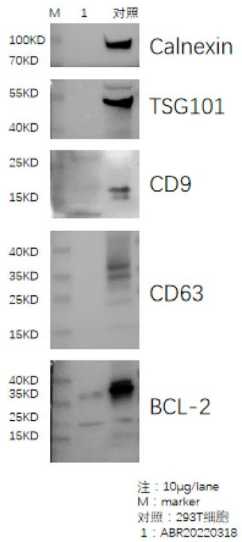

(a) WB detection of extracellular vesicle protein expression

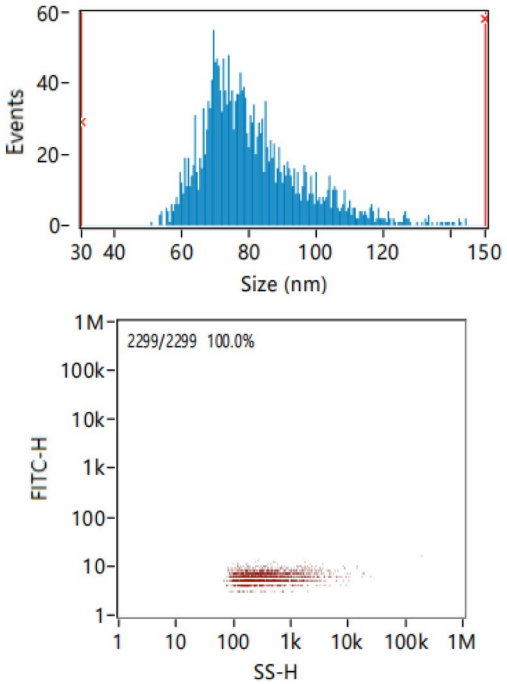

(b) Schematic diagram of particle size and concentration

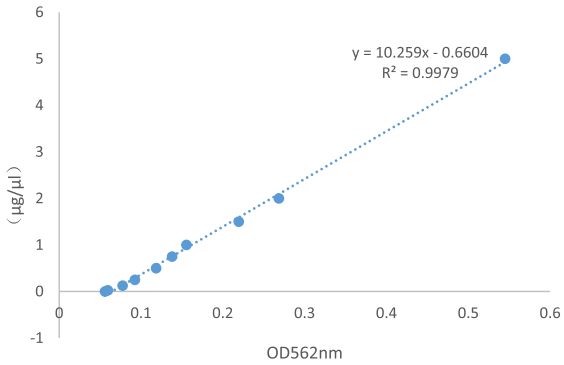

(c) Standard curve for BCA determination of extracellular vesicle protein concentration

(d) electron microscopy images of extracellular vesicles

Fig. 1 **a** WB detection of extracellular vesicle protein expression (**b**) Schematic diagram of particle size and concentration (**c**) Standard curve for BCA determination of extracellular vesicle protein concentration (**d**) electron microscopy images of extracellular vesicles) electron microscopy images of extracellular vesicles

conventional (5% CO_2 and 95% air) or anoxic conditions (80% CO_2 and 20% air). Cell proliferation test was carried out using cell counting kit −8 (CCK8 kit, Kumamoto, Japan).

Cell migration test

The upper surface of Transwell chamber was applied with Matrigel (50 mg/L) at a ratio of 1: 8, and then FN was applied to the lower surface of the chamber, dried and disinfected by ultraviolet rays for 30min. Add 0.1 mL of 1% BSA serum-free medium to each well, and absorb the residual medium after Matrigel was fully infiltrated. Add 0.2 mL (1×10^5) of cell suspension to each hole of precoated culture plate, slowly add 0.5 mL of 10% FBS medium in the lower chamber, and culture in the incubator for 16 h. Add 1 ml of 0.5% crystal violet solution, and wash it. Wipe off the cells on the upper surface of Transwell chamber that had not passed through the basement membrane with a cotton swab, and be careful not

to destroy the basement membrane. Count and compare the cells under the microscope.

Apoptosis experiment

MSCs were trypsinized, collected together and washed, and resuspended with 1×Annexin V binding buffer. Then add 5 μlfitc labeled Annexin V and 5 μl PI solution into 100 μl cell suspension, mix gently, and incubate. And then 400 μl of buffer was joined to the cell suspension, and then the cell suspension was tested by flow cytometry within 1 h.

Skin wound healing model and experimental grouping

Rats were anesthetized by intraperitoneal injection of pentobarbital sodium. And then a full-thickness wound was formed on the back skin. Mesenchymal stem cells and exocrine bodies were suspended and injected into the dermis at four sites around each wound, respectively, and injected into the dermis. In all experiments, mesenchymal stem cells and exosomes were used at the same concentration. After the operation, the wound was overlapped with surgical dressing. D-luciferin (150 mg/kg) was injected at D3, D7 and D10 after operation to stimulate the cell fluorescence (Fig. 2). The images were taken with IVIS Lumina Series III, and the total fluorescence intensity was analyzed with Living Image Software 4.4. The wound area was measured after operation, and the wound healing rate (NIH, USA) was counted by ImageJ software. Rats were killed and skin tissue was collected for further analysis. Rats were separated into the following groups: one group was transplanted with exo@ BCL2 + Luciferase + /GFP + MSCs (group A), one group was transplanted with Luciferase + /GFP + MSCs (group B), one group was transplanted with exo@ wild mouse secretion + Luciferase + /GFP + MSCs (group C), and the fourth wound was blank.

Tissue damage score

On the 7th day, the wound tissue was fixed with 4% paraformaldehyde, embedded in paraffin and cut into 5 μm thick sections. Tissue sections were stained with H&E and Ma Song trichrome. The tissue sections were examined with an optical microscope (Olympus) at magnification of 100 times and 200 times. The sum of the scores obtained by each standard was calculated as the total damage score.

Immunohistochemical analysis

The injured tissues of rats were fixed with 4% paraformaldehyde overnight. After dehydration in 15% and 30% sucrose solutions, the samples were cut into 10mm thick slices. And frozen sections were blocked with 10% BSA,

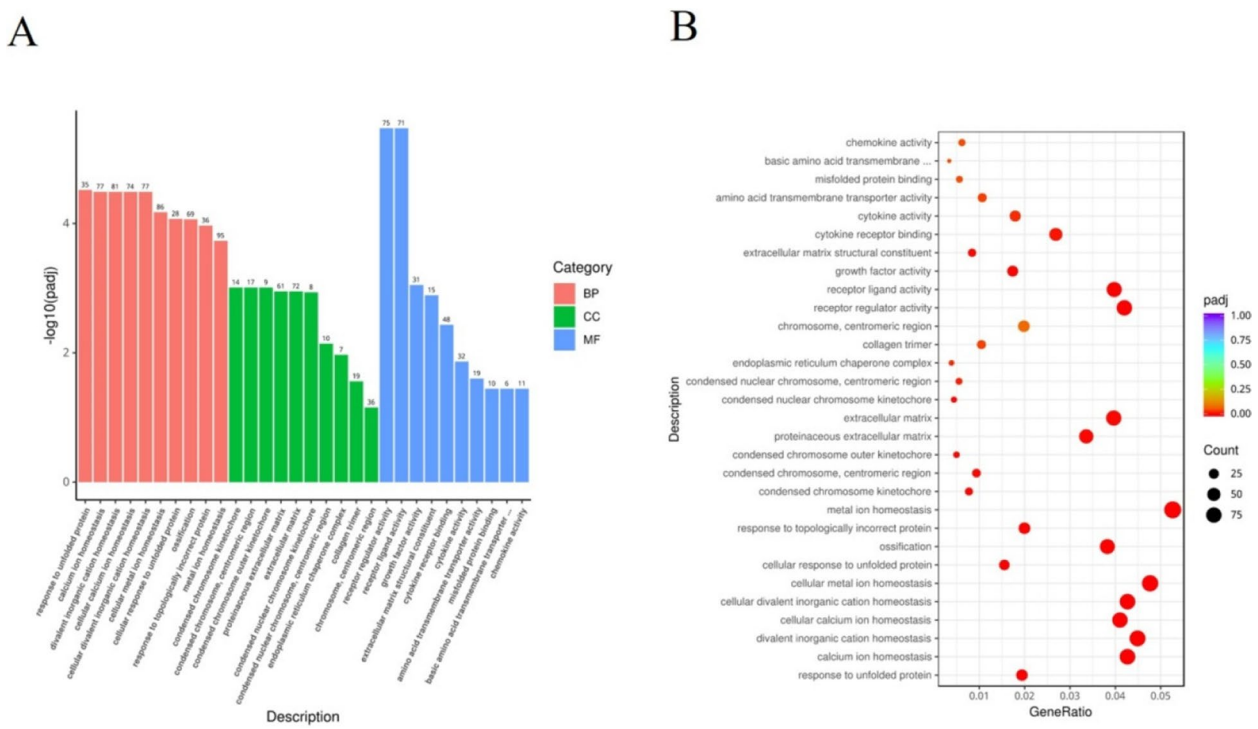

Fig. 2 **A** GO enrichment analysis histogram. Note: In the figure, the abscissa was Go TERM, and the ordinate was the significance level of Go TERM enrichment. Scatter diagram of **B** GO enrichment analysis

incubated with primary antibody KRT14, anti-PCNA, anti-α-SMA and anti-VEGFA overnight at 4℃, and then incubated with secondary antibody. The secondary antibodies include hrp-coupled IgG and Alexa fluorine-coupled IgG (AS014; AS003) and Thermo Fisher Scientific Shier Technology Company.

ELISA analysis

The tissues were isolated 10 days later. Add 1 mM EDTA, 1% Triton X-100, 1 mM benzyl sulfonyl fluoride, 150 mM NaCl, 10 mM Tris and 5 μl/ml protease inhibitor into the lysate. The lysate was centrifuged, and the supernatant was collected. According to the manufacturer's agreement, the cells were measured by rat SDF-1 ELISA kit.

Western blot analysis

Total proteins were extracted from MSCs cell lysates in RIPA lysis buffer including 1% protease and phosphatase inhibitor. Protein was run on SDS polyacrylamide gel, and then transferred to PVDF membrane. The membrane was blocked with 5% BSA for 2 h, and mixed with BCL-2 (1:10 00, AF6139, Affinity), cleaved caspase-3 (1:1000, cell signal technology), caspase-9 (1:1000, #9188, cell signal technology) and caspase-9 at 4℃. #S0001, affinity) was left for 2h. GAPDH antibody was used as control for different loads.

Statistical analysis

All data in this study were processed using SPSS20.0 statistical analysis software (IBM, USA). The measurement data is represented by "mean ± standard deviation" (±s), inter group comparisons are performed using one-way ANOVA or repeated measurement ANOVA, and inter group pairwise comparisons are performed using LSD-t-test. The counting data is expressed as a percentage (%), and inter group comparisons are made using χ^2 Analysis. $P<0.05$ represents a statistically significant difference.

Results

Gene Ontology (GO) analysis

In this study, GO analysis of BCL2-2 was carried out by using LinkOmics online database. The results of molecular function (MF) analysis were shown in Fig. 2A and B. TRIB3 had a positive correlation with NF-kB binding function, tRNA binding function, ubiquitination protein binding function, and an obvious negative correlation with β-catenin binding function and cytokine binding function.

KEGG pathway enrichment analysis results

We used KEGG to study the function of BCL2, and the results were shown in Fig. 3A and B. From KEGG's results, BCL2-2 was closely related to the pathways of Base excision repair, cell cycle and steroid biosynthesis.

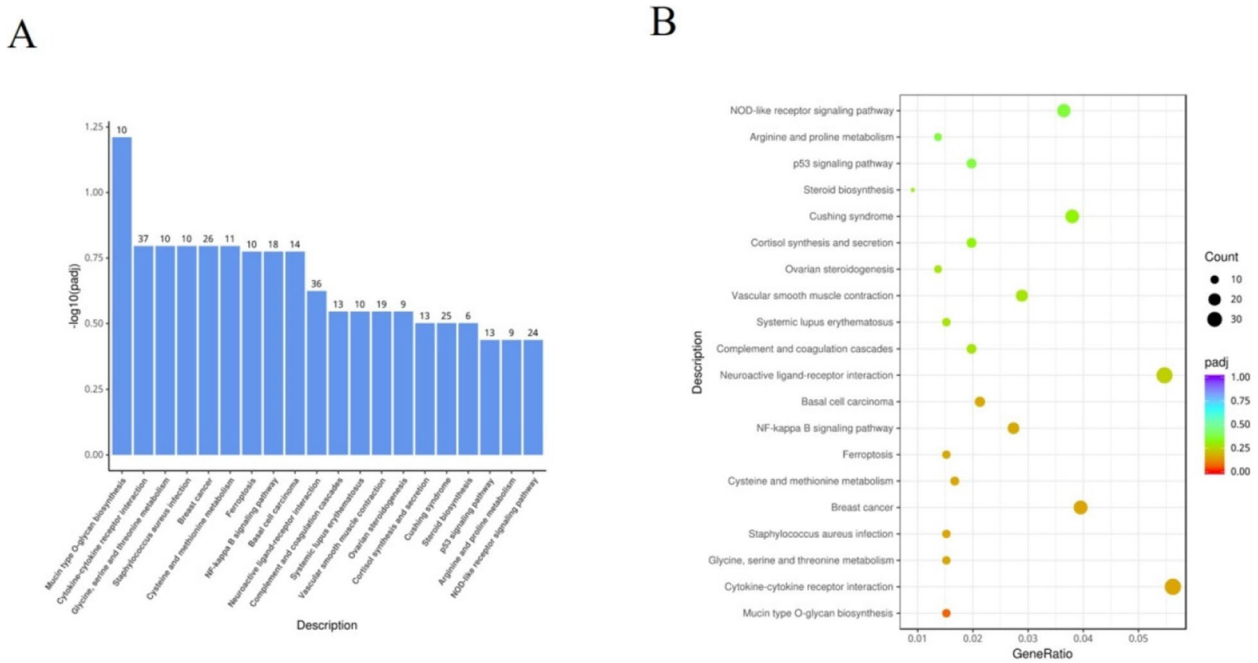

Fig. 3 **A** KEGG enrichment analysis histogram. In the figure, the abscissa was KEGG pathway, and the ordinate was the significance horizontal of pathway enrichment. **B** KEGG enrichment scatter plot

Immunofluorescence staining analysis of MSCs proliferation

The proliferation of MSCs was estimated by immunofluorescence staining. The percentage of Ki67- positive cells in MSC + hypoxia group was lower than MSC + normoxia group ($P < 0.05$), and the percentage of Ki67- positive cells in Exo-BCL-2 + MSC + hypoxia group and MSC + hypoxia group was lower than that in Exo-BCL-2 + MSC + normoxia group and MSC + normoxia group ($P < 0.05$). The percentage of Ki67- positive cells in exo WT + MSC + normoxic group and exo WT + MSC + hypoxic group was lower than that in Exo-BCL-2 + MSC + normoxic group and Exo-BCL-2 + MSC + hypoxic group ($P < 0.05$) (Fig. 4).

BCL-2 exosomes promoted the migration of MSCs in hypoxic environment

The migration ability of MSCs was detected by cell migration test. At 24h and 48h, the migration number of MSCs in MSC + hypoxia group was lower than MSC + normoxia group ($P < 0.05$), and the migration number of MSCs in Exo-BCL-2 + MSC + hypoxia group and MSC + hypoxia group was lower than that in Exo-BCL-2 + MSC + normoxia group and MSC + normoxia group ($P < 0.05$). The migration quantity of MSCs in exo WT + MSC + normoxic group and exo WT + MSC + hypoxic group was lower than that in Exo-BCL-2 + MSC + normoxic group and Exo-BCL-2 + MSC + hypoxic group ($P < 0.05$) (Fig. 5).

BCL-2 exosomes inhibited MSCs apoptosis in hypoxic environment

The activity of MSCs in MSC+ hypoxia group was lower than MSC+ normoxic group ($P<0.05$), and the activity of MSCs in Exo-BCL-2+MSC+ hypoxia group and MSC+ normoxic group was lower than Exo-BCL-2+MSC+ normoxic group and MSC+ normoxic group ($P<0.05$). The apoptosis rate of MSC+ hypoxia group was higher than MSC+ normoxia ($P<0.05$), and that of Exo-BCL-2+MSC+ hypoxia group and MSC+ hypoxia group was higher than that of Exo-BCL-2+MSC+ normoxia group and MSC+ normoxia group ($P<0.05$). The activity of MSCs in exo WT+MSC+ normoxic group and exo WT+MSC+ hypoxic group was lower than that in Exo-BCL-2+MSC+ normoxic group and Exo-BCL-2+MSC+ hypoxic group ($P<0.05$). The apoptosis rate of exo WT+MSC+ normoxic group and exo WT+MSC+ hypoxic group was higher than that of Exo-BCL-2+MSC+ normoxic group and Exo-BCL-2+MSC+ hypoxic group ($P<0.05$) (Fig6).

Expression analysis of apoptosis-related proteins

The protein expressions of caspase3 and caspase9 in MSC+ hypoxia group were higher than those in MSC+ normoxic group ($P<0.05$). The expressions of caspase3 and caspase9 in Exo-BCL-2+MSC+ hypoxia group and MSC+ hypoxia group were higher than Exo-BCL-2+MSC+ normoxicity group and MSC+ normoxicity group ($P<0.05$), while the expressions of caspase3 and caspase9 in Exo-BCL-2+MSC+ normoxicity group were

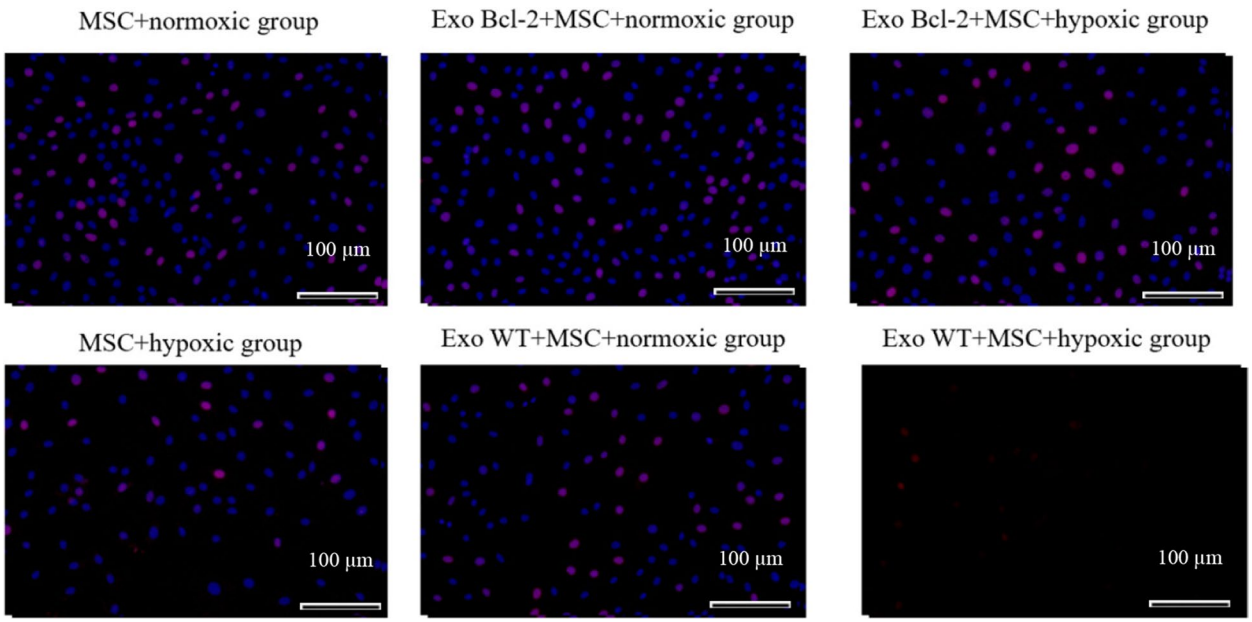

Fig. 4 Immunofluorescence staining analysis

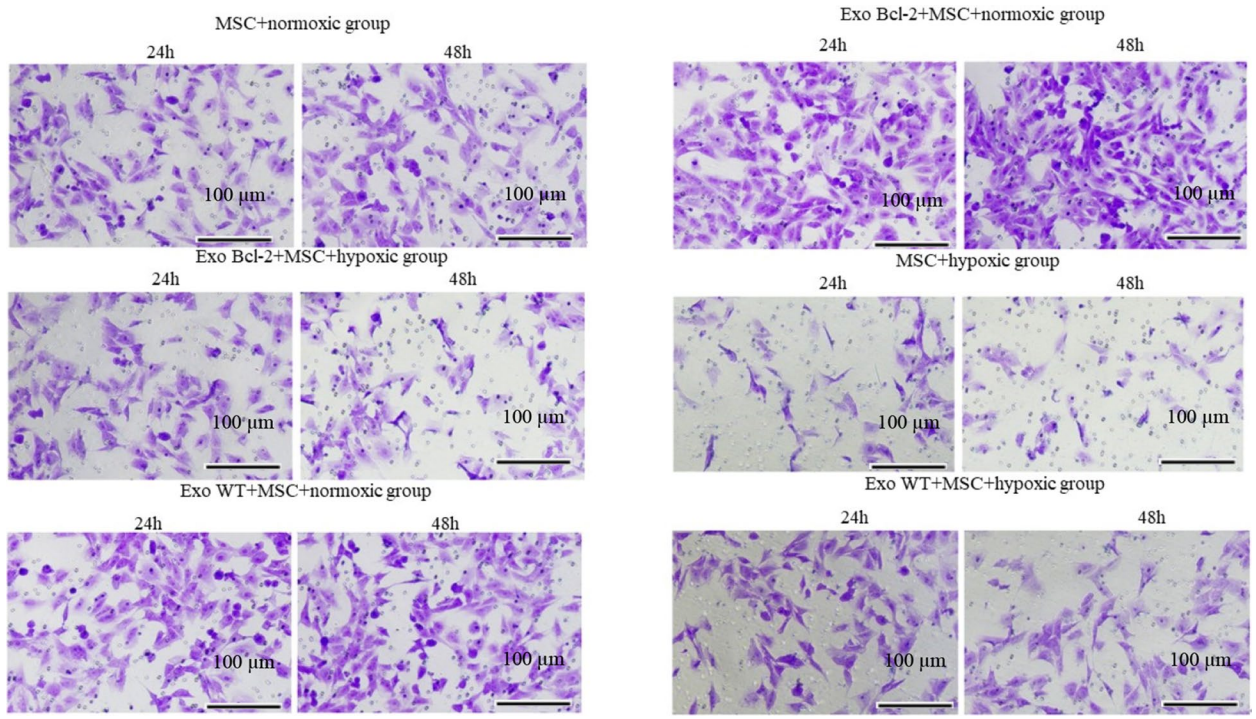

Fig. 5 The migration ability of MSCs was detected by cell migration test

lower than MSC+ normoxicity group (P<0.05). The expressions of caspase3 and caspase9 in exo WT+MSC+ normoxic group and exo WT+MSC+ hypoxic group were higher than Exo-BCL-2+MSC+ normoxic group and Exo-BCL-2+MSC+ hypoxic group (P<0.05). The expression of BCL-2 protein in MSC+ hypoxia group was lower than MSC+ normoxia group (P<0.05), and the expression of BCL-2 protein in Exo-BCL-2+MSC+ normoxia group and MSC+ normoxia group was lower than Exo-BCL-2+and MSC+ normoxia group (P<0.05) (Fig. 7).

Analysis of the rate of wound nonunion in rats

The wounds of rats were recorded by digital camera. On the third day after surgery, there was no statistically significant difference in wound healing rate among the groups of rats (P>0.05). On the 7th and 21st day after operation, the wound healing rates of rats in groups A, B and C were lower than control group (P<0.05), and those in group A were lower than groups B and C (P<0.05) (Fig. 8, Table 1).

Histological staining score

On the 3rd postoperative day, the histological injury scores of group A and group C were lower than control group and group B (P<0.05). On the 7th and 21st postoperative day, the histological injury scores of groups A, B and C were lower than control group (P<0.05) (Fig. 9, Table 2).

Analysis of collagen volume fraction in rat wounds

On the 3rd postoperative day, the collagen volume fraction of wounds in group A was higher than group B, group C and control group (P<0.05), but there was no difference between them (P>0.05). On the 21st postoperative day, the collagen volume fraction of wounds in group A and group C was higher than group B and control group (P<0.05), and on the 21st postoperative day, the collagen volume fraction of wounds in group A and group C was higher than group B and control group (Fig. 10, Table 3).

quantitative analysis of CD31 and PCNA

The protein expressions of CD31 and PCNA in group A, group B and group C were higher than the control group (P<0.05), while those in group A were higher than t group B and group C (P<0.05) (Table 4).

Discussion

The combination of Luciferin and GFP demonstrates enormous potential. Luciferin plays a crucial role in bioluminescence as a substrate for luciferase; GFP, on the other hand, has become an important labeling tool

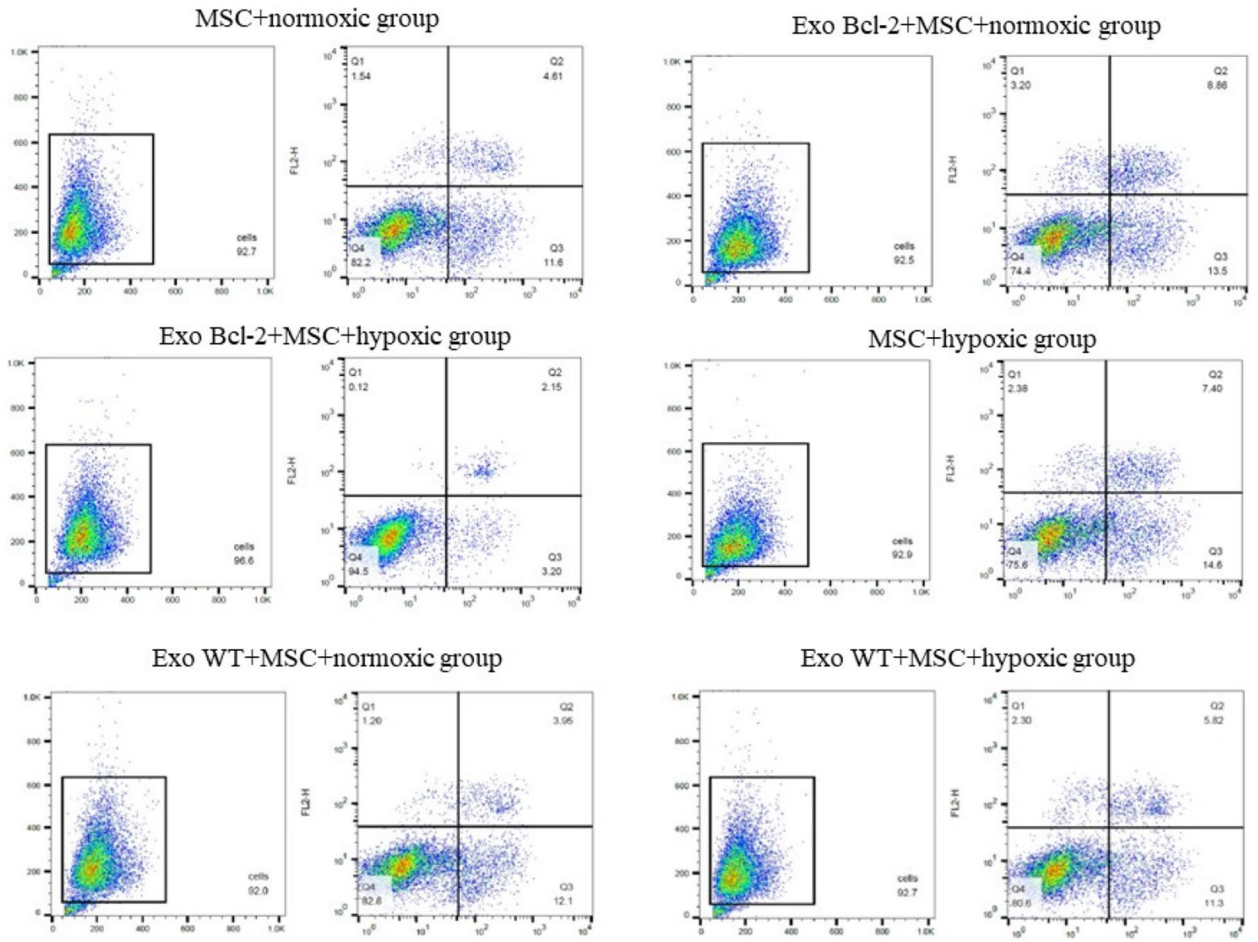

Fig. 6 Apoptosis ability of MSCs was detected by flow cytometry

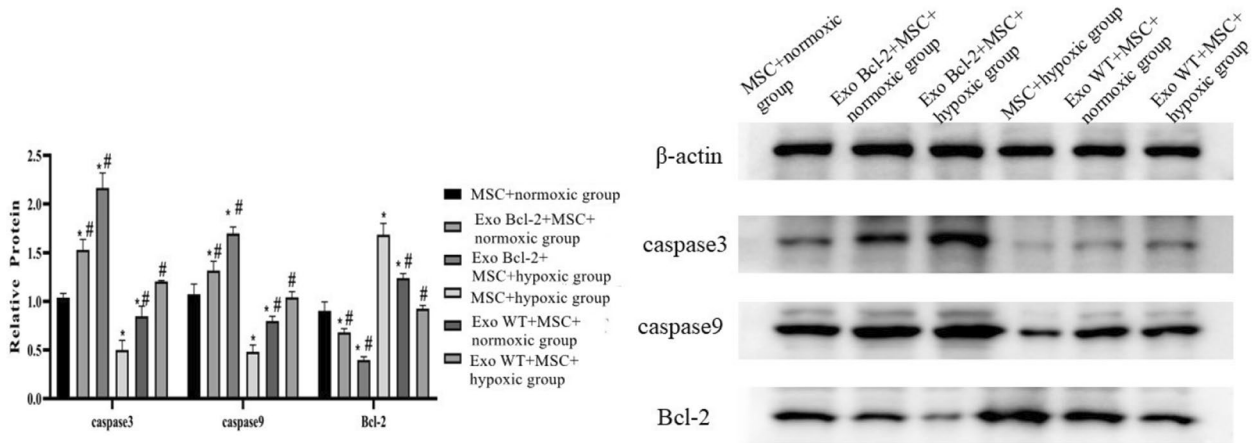

Fig. 7 Western blot analysis of apoptosis-related proteins

due to its unique fluorescence properties. The combination of the two has broad application prospects in fields such as in vivo imaging and drug screening. Luciferin and GFP play important roles in biomedical applications. Luciferin is used for in vivo imaging technology to monitor disease status and drug efficacy in real-time.

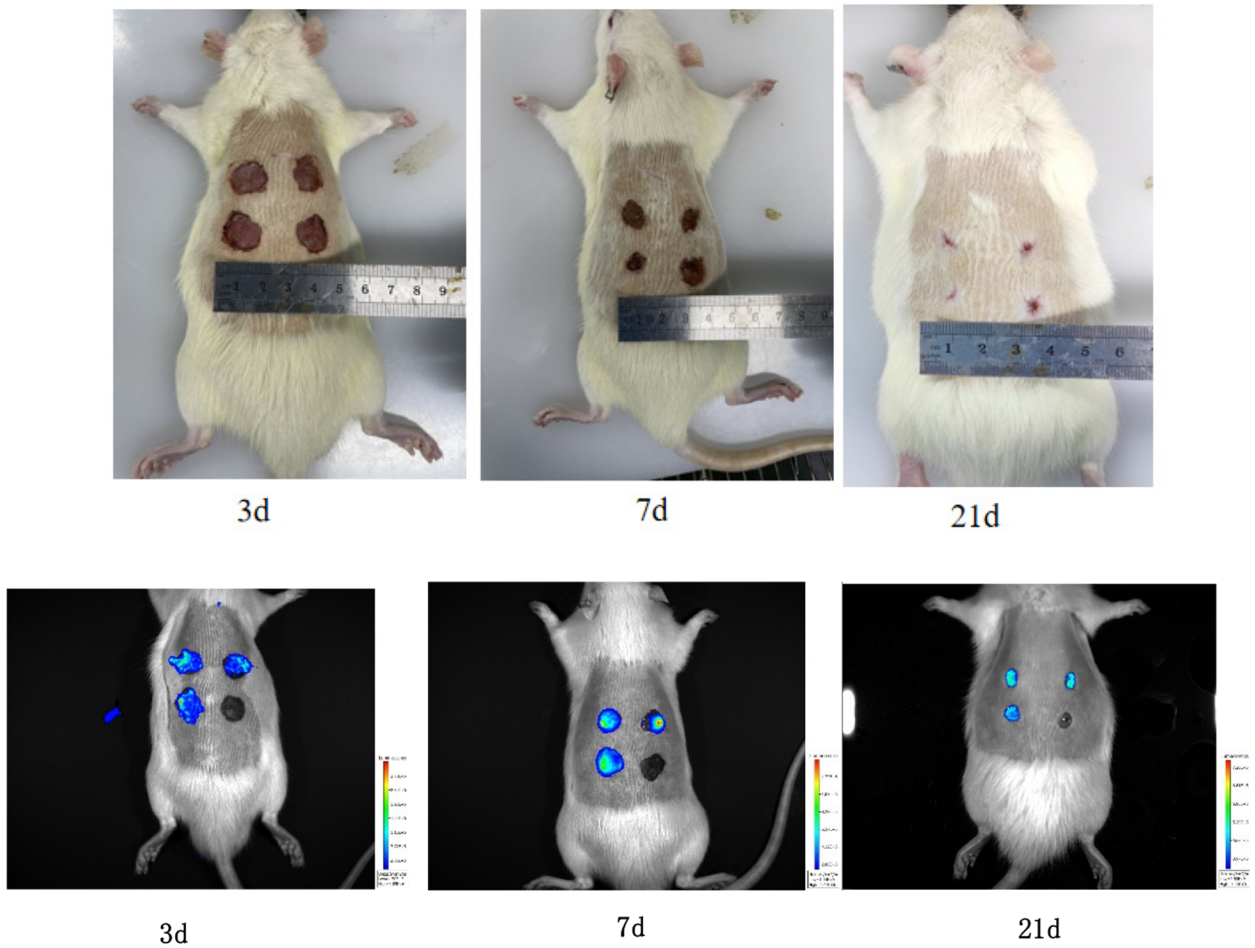

Fig. 8 Analysis of unhealed rate of wound in rats

Table 1 Analysis of Wound Nonunion Rate in Rats (S)

Groups	3d	7d	21d
Control group	63.24 ± 7.44	55.29 ± 4.16	27.46 ± 2.45
Group a	66.19 ± 6.42	36.31 ± 3.28	8.47 ± 1.18
Group b	64.52 ± 6.52	48.62 ± 4.01	23.29 ± 2.11
Group c	61.27 ± 8.35	42.59 ± 3.67	15.54 ± 1.53
F value	5.306	13.278	9.522
P value	0.118	0.001	0.004

Table 2 Histological staining score of rats (S)

Groups	3d	7d	21d
Control group	13.64 ± 1.86	10.22 ± 1.62	8.33 ± 1.17
Group A	8.32 ± 1.32	3.35 ± 0.65	1.25 ± 0.14
Group B	12.58 ± 1.72	9.46 ± 1.51	6.49 ± 1.35
Group C	9.24 ± 1.38	6.38 ± 0.85	4.47 ± 0.70
F value	11.302	9.524	13.918
P value	0.001	0.006	0.001

GFP, as a living reporter protein, is widely used in cell tracking, protein translocation, and enzyme activity observation, and has a profound impact on biomedical research. Luciferin and GFP have shown significant efficacy in treating tumors. A study successfully established lung cancer and liver cancer cell lines using Luciferin and GFP dual labeling technology. Through in vivo imaging systems, real-time and quantitative detection of deep tumor lesions in mice was achieved, providing strong support for tumor treatment.

Some studies have reported that there is no correlation between the horizontal of BCL-2 and the prognosis, but most authors still believe that there is a positive correlation between the increase of BCL-2 protein expression and the good clinical results [18, 19]. This may indicate that the formation and growth of tumor is a complex

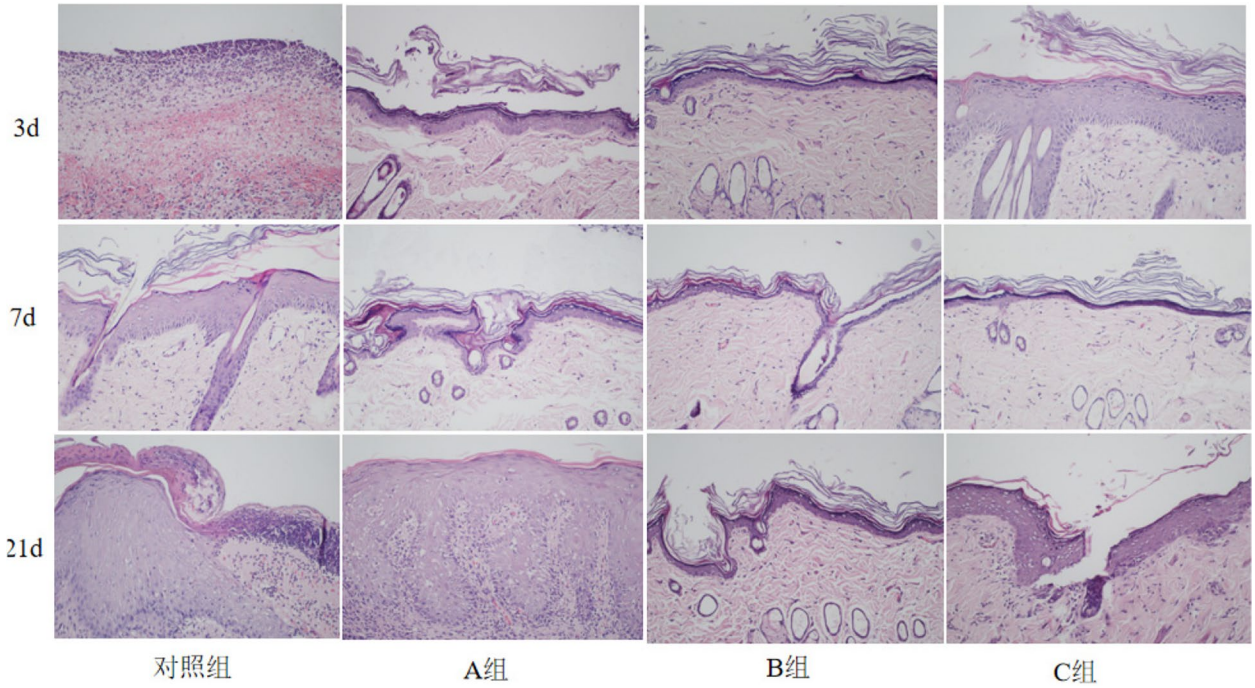

Fig. 9 HE staining of rat tissues

dynamic process, during which cancer cells are constantly changing in many protein syntheses [20]. In order to explore the functional protein and regulatory pathway of BCL-2 in MSC cells, the online database of Link Omics was used for bioinformatics analysis of MSC. The results of molecular function analysis showed that BCL-2 had a positive correlation with NF-kB binding function, with tRNA binding function and ubiquitination protein, and a negative correlation with β-catenin binding function and with cytokine binding function. From KEGG's results, we can see that BCL2-2 was closely related to the pathways of Base excision repair, cell cycle and steroid biosynthesis. BCL-2 is one of the key target genes located downstream of NF-κB. When NF-κ B is activated, it can regulate the transcription of BCL-2 gene and make BCL-2 up-regulated. BCL2 can inhibit the activation of NF-KB and significantly increase the apoptosis rate induced by TNF [21]. Studies have shown that it can inhibit apoptosis by regulating downstream anti-apoptosis genes, and it can inhibit apoptosis by inducing and up-regulating gene expression. When the signal transduction pathway is blocked, the expression level is down-regulated and the inhibition of apoptosis is weakened [17, 22]. To sum up, bioinformatics analysis and previous studies showed that BCL2-2 played a critical function in the process of cell apoptosis and proliferation, and these biological processes go hand in hand the development of tumors.

Table 3 Masson staining was used to estimate the collagen volume fraction (S)

Groups	3d	7d	21d
Control group	32.66 ± 2.27	35.47 ± 2.26	40.62 ± 2.45
Group a	49.30 ± 3.25	54.29 ± 3.31	76.43 ± 6.49
Group b	33.21 ± 2.19	35.16 ± 2.44	52.42 ± 3.29
Group c	34.56 ± 2.08	42.56 ± 3.11	68.51 ± 5.47
F value	11.207	13.665	9.528
P value	0.001	0.001	0.003

The oxygen concentration in vivo under physiological requirement is different from that in vitro, and the normal oxygen condition in vitro cannot simulate the real hypoxia microenvironment in vivo [23]. Studies have discovered that exosomes can enhance the biological function of MSCs and increase its therapeutic effect under hypoxia [24, 25]. This study showed that the exosomes with high expression of BCL-2 can promote MSCs proliferation, increase cell viability and inhibit cell apoptosis in hypoxic environment. In this study, we isolated the exosomes with high expression of BCL-2 from MSCs, and established a normoxic or hypoxic environment model by controlling the oxygen concentration in the culture medium, and then studied the effects of BCL-2 exosomes on the proliferation and migration of MSCs

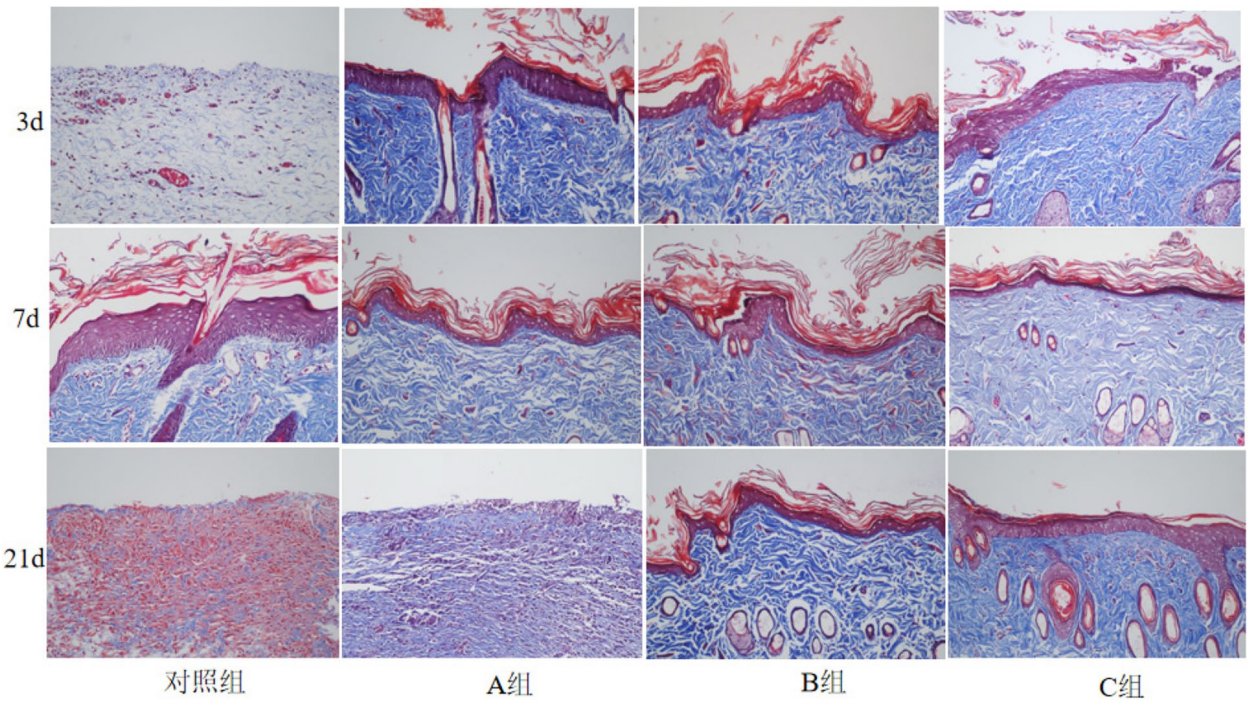

Fig. 10 Masson staining to estimate collagen volume fraction

in different oxygen environments. Immunofluorescence staining, migration test was used to detect the effect of BCL-2 exosomes on MSCs in hypoxic environment, and Western blot was used to test the inhibitory effect of BCL-2 exosomes on MSCs apoptosis in hypoxic environment. The results showed that BCL-2 exosomes could encourage the proliferation of MSCs and inhibit the apoptosis in hypoxic environment. Our research showed that the exosomes with high expression of BCL-2 could promote the proliferation and migration of MSCs in hypoxic environment, promote the lineage differentiation of MSCs, and thus enhance the function of MSCs. At the same time, our research provided new evidence for the possibility of expanding MSCs as a treatment strategy.

In this study, the influence mechanism of MSCs-BCL-2 exosomes on skin repair was discussed by establishing a rat skin injury model. In order to consider the healing function of MSCs-BCL2 exosomes on the healing process of wound surface in rats, the changes of wound size were observed by taking pictures on 3, 7 and 21 days after operation. The wound size of all wounds after treatment was significantly reduced at 7 days and 21 days, while the recovery of wound size in the control group was slow. Among them, exo@BCL2 + Luciferase + / GFP + MSCs group (group A) had the best healing function on the 21st day of the rat wound, the wound was almost completely closed and the hair grew. Consistent with the general observation, the quantitative nonunion rate of wounds showed that the nonunion rate of group A was lower than that of other groups in the whole nonunion process, with the nonunion ratio of 8.47 ± 1.18% on the 21st day, while the final nonunion ratio of other groups were 27.46 ± 2.45% (blank control group), 23.29 ± 2.11% (Luciferase + /GFP + MSCs, B group), and 15.54 ± 1.53%(exo@ wild mouse secretion + Luciferase + / GFP + MSCs, C group). After injection of exosome BCL-2, the wound healing performance of rats in group A and group C was significantly improved than pure MSCs in group B, indicating that exosome BCL-2 can boost the wound healing process through the sustained release of exosome. Different from the control group, which did not form new epidermis, a large number of thinking granulation tissues were formed in the wound space on the 7 th and 21 ST day in groups A, B and C, with more layers. The injured tissue had obvious pathological changes,

Table 4 Quantitative analysis of CD31 and PCNA (S)

Groups	CD31	PCNA
Control group	1.17 ± 0.06	1.15 ± 0.05
Group A	2.31 ± 0.22	2.35 ± 0.23
Group B	1.61 ± 0.12	1.58 ± 0.11
Group C	1.92 ± 0.15	1.88 ± 0.20
F value	11.335	9.142
P value	0.001	0.015

including increased vacuolation, infiltration of inflammatory cells and decreased density of newly formed blood vessels. There was also significant distinguish in tissue damage score between group A and other groups, among which group A was the least, followed by group C, group B and control group respectively. From the analysis of H&E staining, the exosomes released in group A for a long time can be used for wound repair and regeneration more effectively. On the 21st day, the wounds of rats in group A showed rich and well-organized collagen fibers, and the number of collagen fibers raised with the increase of healing time. A large amount of collagen formation during healing is beneficial to the remodeling of collagen matrix and promotes complete healing. The healing tissue is closer to normal skin and the healing effect is better. The volume fraction of collagen showed that MSCs-BCL2 exosomes slow-release system could promote collagen deposition, accelerate skin regeneration and make the wound better or even completely repaired. On the 21st day, skin samples were collected for further histological analysis and the results of skin regeneration were evaluated. The skin structure of MSCs-BCL2 exosomes treatment group was more complete than the other three groups, with newly formed epithelial cells and appendages, and better collagen deposition and tissue. Immunofluorescence staining showed that the expression levels of CD31 and PCNA in group A were better than other three groups. These data showed that the use of NM-Exo can advance the healing of skin wounds and enhance the intensity of angiogenesis more effectively.

Conclusion

To sum up, MSCs-BCL-2 has the characteristics of self-healing, injectability and anti-inflammatory activity, which plays a strong role in promoting the healing of skin injury wounds and can advance the process of wound repair. In a word, this study proves that high expression of BCL-2 exocrine can promote angiogenesis and skin wound healing. The wound treated with MSCs-BCL-2 promotes the formation of new blood vessels and granulation tissue in the wound, the redifferentiation of epithelial cells and the remodeling of collagen, which has a high therapeutic prospect for chronic wounds and skin regeneration.

Supplementary Information

The online version contains supplementary material available at https://doi.org/10.1186/s13036-024-00471-y.

Supplementary Material 1.

Supplementary Material 2.

Supplementary Material 3.

Supplementary Material 4.

Supplementary Material 5.

Supplementary Material 6.

Supplementary Material 7.

Supplementary Material 8.

Acknowledgements
Not applicable.

Authors' contributions
YW, GL, GL, YP and ZL designed and wrote the original manuscript, performed theexperiments and wrote the original manuscript, administered and coordinated the whole study project. All authors have read and agreed to the published version of the manuscript.

Funding
Not applicable.

Data availability
The original contributions presented in the study are included in the article.

Declarations

Ethics approval and consent to participate
All experimental protocols were approved by the Animal Ethics Committee of the Shanghai East Hospital of Tongji University. All methods were carried out in accordance with relevant guidelines and regulations. All methods are reported in accordance with ARRIVE guidelines

Consent to publication
Not applicable.

Competing interests
The authors declare no competing interests.

Author details
[1]Department of Traumatic Clinic, Shanghai East Hospital of Tongji University, Shanghai 200120, China.

Received: 8 September 2024 Accepted: 4 December 2024
Published online: 17 January 2025

References

1. Walsh GM, Dewson G, Wardlaw AJ, Levi-Schaffer F, Moqbel R. Expression of BCL-2 and Its Homologues in Human Eosinophils. 2019;97:701–9.
2. Kallepu S, Kavitha M, Yeeravalli R, Manupati K, Jadav SS, Das A, et al. Total Synthesis of DesmethylJahanyne and Its Lipo-Tetrapeptide Conjugates Derived from Parent Skeleton as BCL-2-Mediated Apoptosis-Inducing Agents. ACS Omega. 2018;3:63–75.
3. Opferman JT, Kothari A. Anti-apoptotic BCL-2 family members in development. Cell Death Differ. 2018;25:37–45.
4. Maciel-Silva P, Caldeira I, Icaro D, Carreira A, Siqueira FR, Antonioli E, et al. FAM3B/PANDER inhibits cell death and increases prostate tumor growth by modulating the expression of BCL-2 and Bcl-XL cell survival genes. BMC Cancer. 2018;18:90.
5. Khan WS, Hardingham TE. Mesenchymal stem cells, sources of cells and differentiation potential. J Stem Cells. 2012;7:75–85.
6. Nuri MM, Hafeez S. Autologous bone marrow stem cell transplant in acute myocardial infarction. J Pak Med Assoc. 2012;62:2–6.
7. Wang S, Qin X, Sun D, et al. Effects of hepatocyte growth factor overexpressed bone marrow-derived mesenchymal stem cells on prevention

from left ventricular remodelling and functional improvement in infarcted rat hearts. Cell Biochem Funct. 2012;30:574–81.
8. Sinha K, Das J, Pal PB, et al. Oxidative stress: the mitochondria-dependent and mitochondria-independent pathways of apoptosis. J Arch Toxicol. 2013;87:1157–80.
9. Zhang S, Chuah SJ, Lai RC, et al. MSC exosomes mediate cartilage repair by enhancing proliferation, attenuating apoptosis and modulating immune reactivity. J Biomater. 2018;156:16–27.
10. Lu HH, Li YF, Sheng ZQ, et al. Preconditioning of stem cells for the treatment of myocardial infarction. Chin Med J (Engl). 2012;125:378–84.
11. Wang F, Zhou H, Du Z, et al. Cytoprotective effect of melatonin against hypoxia/serum deprivation-induced cell death of bone marrow mesenchymal stem cells in vitro. Eur J Pharmacol. 2015;748:157–65.
12. Schneider A, Simons M. Exosomes: vesicular carriers for intercellular communication in neurodegenerative disorders. Cell Tissue Res. 2013;352(1):33–47.
13. Bailey AJM, Tieu A, Gupta M, et al. Mesenchymal Stromal Cell-derived Extracellular Vesicles in Preclinical Animal Models of Tumor Growth: Systematic Review and Meta-analysis. Stem Cell Rev Rep. 2022;18:993–1006.
14. Cheng YQ, Wang SB, Liu JH, et al. Modifying the tumour microenvironment and reverting tumour cells: New strategies for treating malignant tumours. Cell Prolif. 2020;53: e12865.
15. Fu M, Xie D, Sun Y, et al. Exosomes derived from MSC pre-treated with oridonin alleviates myocardial IR injury by suppressing apoptosis via regulating autophagy activation. J Cell Mol Med. 2021;25:5486–96.
16. Gao W, He R, Ren J, et al. Exosomal HMGB1 derived from hypoxia-conditioned bone marrow mesenchymal stem cells increases angiogenesis via the JNK/HIF-1α pathway. FEBS Open Bio. 2021;11:1364–73.
17. Liu X, Li X, Zhu W, et al. Exosomes from mesenchymal stem cells overexpressing MIF enhance myocardial repair. J Cell Physiol. 2020;235:8010–22.
18. Hu J, Chen X, Li P, et al. Exosomes derived from human amniotic fluid mesenchymal stem cells alleviate cardiac fibrosis via enhancing angiogenesis in vivo and in vitro. Cardiovasc DiagnTher. 2021;11:348–61.
19. Huang P, Wang L, Li Q, et al. Atorvastatin enhances the therapeutic efficacy of mesenchymal stem cells-derived exosomes in acute myocardial infarction via up-regulating long non-coding RNA H19. Cardiovasc Res. 2020;116:353–67.
20. Kong LY, Li Y, Rao DY, et al. miR-666-3p Mediates the Protective Effects of Mesenchymal Stem Cell-derived Exosomes Against Oxygen-glucose Deprivation and Reoxygenation- induced Cell Injury in Brain Microvascular Endothelial Cells via Mitogen-activated Protein Kinase Pathway. CurrNeurovasc Res. 2021;18:20–77.
21. Kong LY, Liang MY, Liu JP, et al. Mesenchymal Stem Cell-derived Exosomes Rescue Oxygen-Glucose Deprivation-induced Injury in Endothelial Cells. CurrNeurovasc Res. 2020;17:155–63.
22. Lee CW, Chen YF, Hsiao AW, et al. Demystifying the long noncoding RNA landscape of small EVs derived from human mesenchymal stromal cells. J Adv Res. 2022;39:73–88.
23. Qiu X, Liu J, Zheng C, et al. Exosomes released from educated mesenchymal stem cells accelerate cutaneous wound healing via promoting angiogenesis. Cell Prolif. 2020;53: e12830.
24. Ren S, Wang C, Guo S. Review of the Role of Mesenchymal Stem Cells and Exosomes Derived from Mesenchymal Stem Cells in the Treatment of Orthopedic Disease. Med Sci Monit. 2022;28: e935937.
25. Song Y, Wang B, Zhu X, et al. Human umbilical cord blood-derived MSCs exosome attenuate myocardial injury by inhibiting ferroptosis in acute myocardial infarction mice. Cell Biol Toxicol. 2021;37:51–64.

Publisher's Note